CISM COURSES AND LECTURES

Series Editors:

The Rectors
Friedrich Pfeiffer - Munich
Franz G. Rammerstorfer - Wien
Jean Salençon - Palaiseau

The Secretary General
Bernhard Schrefler - Padua

Executive Editor
Paolo Serafini - Udine

The series presents lecture notes, monographs, edited works and proceedings in the field of Mechanics, Engineering, Computer Science and Applied Mathematics.
Purpose of the series is to make known in the international scientific and technical community results obtained in some of the activities organized by CISM, the International Centre for Mechanical Sciences.

INTERNATIONAL CENTRE FOR MECHANICAL SCIENCES

CISM

WAVE PROPAGATION IN LINEAR AND NONLINEAR PERIODIC MEDIA

ANALYSIS AND APPLICATIONS

EDITED BY

FRANCESCO ROMEO
UNIVERSITY "LA SAPIENZA", ROME, ITALY

MASSIMO RUZZENE
GEORGIA INSTITUTE OF TECHNOLOGY, ATLANTA, USA

This volume contains 175 illustrations

SPIN 86122731

All contributions have been typeset by the authors.

PREFACE

Periodic structural configurations are ubiquitous: many heterogeneous structures and materials, both man-made and naturally occurring, feature geometry, micro-structural and/or materials properties that vary periodically in space. The classes of periodic materials and structures span a wide range of length scales, and a broad range of applications. Periodic trusses, periodically stiffened plates, shells and beam-like assemblies can be found for example in many civil, aerospace, mechanical and ship constructions. Their introduction is mostly motivated by structural strength and weight requirements, however recent studies have shown how the periodicity can be exploited to attenuate, isolate and localize vibrations. Such studies explore the unique ability of periodic assemblies to impede the propagation of elastic waves over specified frequency bands, within which strong attenuation of vibration and radiated noise can be achieved. The attenuation levels that can be obtained through tailored structural periodicity far exceed the performance of most energy dissipation and damping mechanisms. For this reason, passive, active and hybrid periodic structural configurations are being proposed for the reduction of vibration transmission and structure-born as well as airborne noise. In addition, the understanding of the dynamics of periodic structures is essential for the analysis of bladed disc assemblies which are found in turbo machinery and in turbines for energy generation where failure mechanisms due to localization phenomena may occur. At much smaller scales, extensive research is being devoted to the analysis and design of phononic metamaterials for a variety of applications. Phononic metamaterials are essentially periodic structural configurations obtained through composite designs featuring periodic modulations of mass and stiffness properties, or elastic lattice structures. Gigahertz communication devices, such as mobile phones, use phononic-based systems for their low-power filtering characteristics. Many sensing devices based on resonators, acoustic logic ports, and surface acoustic wave-based filters rely on the unique band gap characteristics of periodic phononic materials. These properties are associated with the destructive and constructive interference of acoustic waves originating at the periodic interfaces, which produce frequency band of strong attenuation of acoustic waves (band gaps). Depending on the

inclusions, geometry, and elastic properties, one can design for specific band gaps. In photonic crystals, periodic modulations of the dielectric properties of a medium allow guiding, focusing and steering of electromagnetic waves. Properties modulations and engineered anisotropy in heterogeneous media can also produce negative refractive indexes, both in photonics as well as in phononic metamaterials, which lead to super-lensing or super-focusing characteristics. Dispersion of waves in media with boundaries or built-in micro-structure is a fundamental phenomenon, which occurs in problems of acoustics, models of water waves, simple systems involving onedimensional harmonic oscillators, as well as complex elastic systems. Moreover, enhanced transmission based on formation of defect modes within an interface plays a crucial role in a wide range of practical applications involving filtering and polarisation of waves of different physical origins. Other potential implications of the acoustic wave guiding technology include active sensing of structural integrity, smart sensing of environment, dissipation of high frequency modes of vibration to enhance vehicle performance or stealth, as well as applications to the medical field for sensing or diagnostic applications. Complex dynamical phenomena may be encountered in nonlinear periodic media such as the existence of energy- depended nonlinear propagation regions. Depending on substructure coupling, distinctly nonlinear dynamical phenomena can arise, such as wave localization and solitary waves. Potential applications of such phenomena are currently investigated in the MEMS context, where arrays of coupled micro/nanoresonators have been recently proposed. The CISM course "Wave propagation in linear and nonlinear periodic media: analysis and applications" was an opportunity to combine the material issued from such a variety of applications aiming to present both the theoretical background and an overview of the state-of-the art in wave propagation in linear and nonlinear periodic media in a consistent lecture format. The course is intended for doctoral and postdoctoral researchers in civil and mechanical engineering, applied mathematics and physics, academic and industrial researchers, which are interested in conducting research in the topic. The opening chapter, by A.B. Movchan, M. Brun and N.V. Movchan, gives an overview of some mathematical models of wave propagation in structured media, with the emphasis on dispersion and enhanced transmission through structured interfaces.

Chapter 2, by L. Airoldi, M. Senesi and M. Ruzzene, presents two examples of internally resonating metamaterials whose behavior is based on multi-field coupling. The first part of the chapter is devoted to the analysis of a one-dimensional waveguide with a periodic array of shunted piezoelectric patches. The second part presents the study of piezoelectric superlattices as an additional example of an internally resonant metamaterial. Topology optimization relevant to problems in vibration and wave propagation is then addressed in Chapter 3 by J. S. Jensen; in this chapter the steady-state optimization procedure for dynamical systems is extended to a nonlinear wave propagation problem and then the topology optimization procedure is applied to transient dynamic simulations for which the optimized material distributions may vary in time. In Chapter 4, by F. Romeo, the dynamic behaviour of continuous and discrete models of both linear and nonlinear periodic mechanical systems are dealt with by means of maps. At first, linear problems consisting of general multi-coupled periodic systems are presented and they are handled with linear maps, namely the transfer matrices of single units. Afterwards, a perturbation method is applied to the transfer matrix of a chain of continuous nonlinear beams while nonlinear maps are considered to address chains of nonlinear oscillators. In the closing chapter, by A. Vakakis, analytical methodologies for analyzing waves in weakly or strongly nonlinear periodic media are discussed. The generation of spatial chaos in ordered granular media, which are a special class of spatially periodic, highly discontinuous and strongly nonlinear media is eventually highlighted.

CONTENTS

Waves and defect modes in structured media

A.B. Movchan[a], M. Brun[b], N.V. Movchan[a]

[a] Department of Mathematical Sciences,
University of Liverpool, Liverpool L69 7ZL, U.K.

[b] Department of Structural Engineering,
University of Cagliari, Cagliari I-09123, Italy

Abstract. The paper gives an overview of some mathematical models of wave propagation in structured media, with the emphasis on dispersion and enhanced transmission through structured interfaces. We begin with conventional definitions and classical models of dispersive waves, discuss lattice approximations and then show the results of the recent work on modelling of waves interacting with a structured stack acting as a polarizer of elastic waves. Special attention is given to the resonance modes which may enhance transmission across the structured stack. The analytical work is accompanied by numerical simulations.

0.1 Introduction

Dispersion of waves in periodic inhomogeneous media is important in many problems of physics, mechanics and engineering. A special mention should be given to theoretical and experimental studies of photonic band gap materials (see, for example, Yablonovitch (1987, 1993)). Scalar models for Bloch waves in periodic lattices are discussed in Brillouin (1953), Maradudin *et al.* (1963) and Kunin (1975). This theory naturally extends to vector problems of elasticity. In particular, dispersion of elastic waves in lattice systems of different types has been analysed in Martinsson and Movchan (2003), Jensen (2003), Cai *et al.* (2005).

Dynamic lattice Green's functions in the propagating frequency range were analysed in Martin (2006), whereas the stop band Green's functions and exponentially localised "defect modes" were studied in Movchan & Slepyan (2007).

In wave propagation problems for structured media, the classical homogenisation approaches have limitations when the wavelength is comparable with the characteristic size of elements of the structure, such as a typical

size of the elementary cell. In particular, this appears to be important in the analysis of wave interaction with finite width structured interfaces. Several classes of *non-local structured interfaces* were analysed in Bigoni and Movchan (2002) in static and dynamic configurations, which also included semi-discrete systems incorporating both continuous parts and a lattice. Brun et al. (2010a) have addressed anomalies in transmission of slow waves through dynamic structured interface of finite width. Brun et al. (2010b) addressed the case of a shear-type structured interface excited by a plane pressure wave at an oblique incidence, and this paper also shows that the shear-type interface could serve as a polariser.

In the present paper we aim to discuss the dispersion, polarisation and filtering of waves from a common perspective, with the emphasis on the dynamics of structured interfaces and connections between discrete and high-contrast continuous systems. The structure of the paper is as follows. We begin with the discussion of the fundamental phenomena, such as wave dispersion, and in Section 0.2 we show a very intuitive textbook example of dispersive waves, derived in the framework of the linear water wave theory. Section 0.3 includes the classical notion of Bloch-Floquet waves and an explicit analytical study of wave dispersion in one-dimensional lattice systems. Furthermore, this section also introduces the high-contrast continuous systems, with the emphasis on the lattice approximations of the dispersion equations in such systems. An example of the transmission problem for a one-dimensional finite width structured interface is discussed in Section 0.5, where it is shown that an irregularity within the structure of the interface may lead to an enhanced transmission for waves of certain frequency. A full vector problem of elasticity is described in Section 0.6 for plane elastic waves interacting with a shear-type structured interface; the finite width interface contains several parallel elastic bars, whose motion is preferential in the direction along the interface. This creates an effect of polarization, and we also describe an enhanced transmission for waves of certain frequencies.

0.2   Wave dispersion

This introductory section discusses some classical examples of dispersive waves, i.e. the waves whose speeds are different for different frequencies. Here we refer to the linear water wave theory, which is very well known in linearised models of fluid flow (see, for example, Billingham & King (2001), Ockendon *et al.* (2003)). The second example, included in Section 0.3, is a one-dimensional lattice system, known from classical texts (see, for example, Kittel (1996) and Brillouin (1953)). The dispersion relations are written in an explicit form, and formation of a stop band is discussed for

heterogeneous systems. An asymptotic model is given for a high-contrast stratified structure in Section 0.3. Following Movchan *et al.* (2002a) we show the lattice approximation of such a system, which is capable of reproducing the dynamic response of the heterogeneous continuum system in the low frequency range.

Formulation for linear water waves

One of the straightforward examples is based on the linear theory of waves propagating along the surface of an incompressible inviscid fluid of the uniform density. For convenience, we call such a fluid "water". The continuity equation and the equation of motion for the velocity $\mathbf{u}$ and pressure p have the form

$$\nabla \cdot \mathbf{u} = 0 \qquad , \qquad (1)$$

$$\frac{\partial \mathbf{u}}{\partial t} + (\mathbf{u} \cdot \nabla)\mathbf{u} + \frac{1}{\rho}\nabla p = \mathbf{F} \qquad , \qquad (2)$$

where $\mathbf{F}$ is the body force density, ρ is the mass density and t is time. In particular, if the body force represents gravity we have $\mathbf{F} = -g\mathbf{e}^{(3)}$, and

$$\mathbf{F} \quad = \nabla\Xi \text{ with } \Xi \quad = -gx_3, \qquad (3)$$

where g is a positive constant (normalised gravitational acceleration).

Assuming that the fluid flow is irrotational and using the notation ϕ for the velocity potential we have $\mathbf{u} = \nabla\phi$. Hence according to (1) the function ϕ is harmonic

$$\nabla^2 \phi = 0. \qquad (4)$$

The non-linear term in (2) becomes

$$\{(\mathbf{u} \cdot \nabla)\mathbf{u}\}_i = \sum_j u_j u_{i,j} = \sum_j \phi_{,j}\phi_{,ij} = \frac{1}{2}|\nabla\phi|^2_{,i} \qquad (5)$$

Thus, (2) may be written as

$$\nabla\left(\frac{\partial \phi}{\partial t} + \frac{1}{2}|\nabla\phi|^2 + \frac{p}{\rho} + gx_3\right) = 0,$$

which leads to Bernoulli's equation

$$\frac{\partial \phi}{\partial t} + \frac{1}{2}|\nabla\phi|^2 + \frac{p}{\rho} + gx_3 = f(t), \qquad (6)$$

where $f(t)$ is a function of t only.

Next, we discuss the boundary conditions. The schematic diagram and relevant notations are shown in Fig. 1. It is assumed that the bottom surface S_1 of the channel is fixed and hence the normal component of the velocity equals zero, that is

$$\mathbf{u} \cdot \mathbf{n} = 0 \quad \text{on} \quad S_1. \tag{7}$$

Free surface $p = p_0 = \text{const}$

S_2

Water

Fixed bottom surface S_1
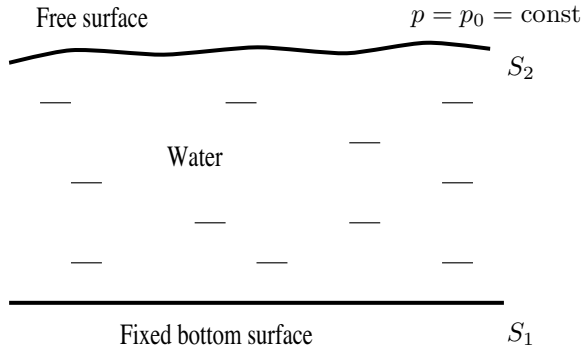
Figure 1. Surface water waves in a flow of finite depth.

It is also assumed that the upper surface S_2 is characterised by the equation

$$x_3 = \zeta(x_1, x_2, t),$$

and there is no variation in pressure on S_2:

$$p = p_0 = \text{const} \quad \text{on} \quad S_2.$$

Hence, according to (6) on the free surface we have

$$\frac{\partial \phi}{\partial t} + \frac{1}{2}|\nabla \phi|^2 + \frac{p_0}{\rho} + g\zeta(x_1, x_2, t) = f(t), \quad \text{as } x_3 = \zeta(x_1, x_2, t). \tag{8}$$

This is accompanied by the identity

$$u_3 = \frac{dx_3}{dt} = \frac{d\zeta}{dt} = \frac{\partial\zeta}{\partial t} + u_1\frac{\partial\zeta}{\partial x_1} + u_2\frac{\partial\zeta}{\partial x_2} \quad \text{on} \quad x_3 = \zeta(x_1, x_2, t). \quad (9)$$

In the linear approximation, we simplify the problem by addressing the case when $|\mathbf{u}|$ and the surface fluctuations are small.

In particular, if the unperturbed surface is $x_3 = h$, then for the free surface we can write

$$\phi(\mathbf{x}, t) = \phi(x_1, x_2, \zeta(x_1, x_2, t), t) =$$
$$= \phi(x_1, x_2, h, t) + (\zeta - h)\phi_{,3}(x_1, x_2, h, t) + \dots$$

To the leading order approximation, the relations (8), (9) are set on the unperturbed surface $x_3 = h$. The second-order term $\frac{1}{2}|\nabla \cdot \phi|^2$ is neglected, and equation (8) becomes

$$\frac{\partial\phi}{\partial t} + \left(\frac{p_0}{\rho} - f(t) + gh\right) + g(\zeta - h) = 0.$$

Since the term $\left(\frac{p_0}{\rho} - f(t) + gh\right)$ is a function of t only, it does not give any contribution to $\mathbf{u}$, and may be "absorbed" into $\frac{\partial\phi}{\partial t}$. Thus, the velocity potential ϕ can be chosen in such a way that

$$\frac{\partial\phi}{\partial t} + g(\zeta - h) = 0 \quad \text{on} \quad x_3 = h. \quad (10)$$

By neglecting the second-order terms $\phi_{,1}$, $\zeta_{,1}$ and $\phi_{,2}$, $\zeta_{,2}$ in (9), involving the partial derivatives of ζ and ϕ, we deduce that to the leading order

$$\frac{\partial\phi}{\partial x_3} = \frac{\partial\zeta}{\partial t} \quad \text{on} \quad x_3 = h, \quad (11)$$

and therefore equations (10), (11) yield

$$\frac{\partial^2\phi}{\partial t^2} + g\frac{\partial\phi}{\partial x_3} = 0 \quad \text{on} \quad x_3 = h. \quad (12)$$

Thus, in the "ocean" with the flat bottom surface $x_3 = 0$ and the unperturbed upper surface $x_3 = h$, the linearized formulation for the velocity potential ϕ is comprised of Laplace's equation (4) within the fluid layer $0 < x_3 < h$, the boundary condition $\mathbf{n} \cdot \nabla\phi = 0$ at the fixed bottom surface $x_3 = 0$, and the "free surface" boundary condition (12). Note that this formulation involves the second-order time derivative of the velocity potential on the upper free surface. In turn, after evaluation of ϕ, the "wave profile" on the free upper surface is defined by (10).

Deep water waves versus waves in shallow water

Consider a surface water wave, with the straight front perpendicular to the x_1-axis. We seek solutions independent of x_2 with the velocity potential

$$\phi = \phi(x_1, x_3, t). \tag{13}$$

It is convenient to work with the complex potential Ψ of the form

$$\Psi = W(x_3)e^{-i(\omega t - kx_1)},$$

and assume that $\phi = \Re e\Psi$. Considering a harmonic solution (i.e. $\nabla^2\Psi = 0$) we obtain

$$W'' - k^2 W = 0,$$

which yields

$$W = C_1 \cosh(kx_3) + C_2 \sinh(kx_3).$$

The boundary condition at the bottom surface ($x_3 = 0$) leads to $W'(0) = 0$, and hence $C_2 = 0$ and

$$\Psi = C_1 \cosh(kx_3)e^{-i(\omega t - kx_1)}. \tag{14}$$

In turn, the free surface condition

$$\left(\frac{\partial^2\Psi}{\partial t^2} + g\frac{\partial\Psi}{\partial x_3}\right)\Bigg|_{x_3=h} = 0 \tag{15}$$

becomes

$$\{-\omega^2 C_1 \cosh(kh) + gkC_1 \sinh(kh)\}e^{-i(\omega t - kx_1)} = 0,$$

which simplifies to the form

$$gk\tanh(kh) = \omega^2. \tag{16}$$

Equation (16) relates the wave number k and the radian frequency ω, and thus the wave speed $c = \frac{\omega}{k}$ is in general frequency dependent. This shows that the water surface waves are *dispersive*. The relation (16) is called the *dispersion equation*.

We would like to note two important particular cases, which are

(a) Deep water, when the non-dimensional quantity $kh \gg 1$ is large, and hence $\tanh(kh) \simeq 1$. Thus to leading order the dispersion equation (16) yields

$$\omega^2 = gk.$$

In this case, the wave speed increases when the frequency decreases, i.e. $c = g\omega^{-1}$, which is fully consistent with the physical observation that low frequency waves in the ocean propagate faster than the high frequency ripples.

(b) Shallow water, when $kh \ll 1$, and hence $\tanh(kh) \sim kh$. In this case, to leading order the dispersion equation (16) takes the form

$$\omega^2 = gk^2h,$$

which implies $c = \sqrt{gh}$. In the framework of this approximation, the wave speed in shallow water is frequency independent and hence the shallow water waves can be treated as non-dispersive.

It is noted that the dispersion of surface water waves in the above illustrative example is linked to the boundary condition (12), which involves the second-order time derivative of the velocity potential.

The phenomenon of wave dispersion can also be observed in simple periodic structures. Conventionally, dispersion diagrams are used to describe the change in frequency with the wave number, which will be illustrated in the next section.
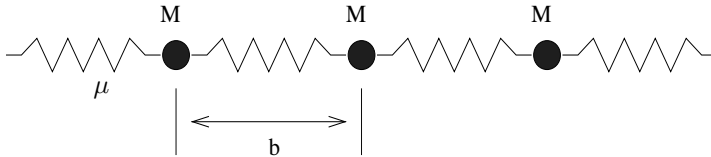
Figure 2. The one-dimensional spring-mass periodic structure.

0.3 Bloch-Floquet waves in periodic structures

A Bloch-Floquet wave in a periodic system is an object discussed in the classical texts, such as Kittel (1996) and Brillouin (1953). We give an outline of elementary examples incorporating a time-harmonic motion of a one-dimensional periodic lattice, consisting of rigid particles connected by

massless springs. The sketch of such a system is shown in Fig. 2. First, we consider the case when all particles have the same mass M, which will be followed by the comparative analysis of the inhomogeneous lattice involving particles of different mass. The separation between neighbouring masses is set to be unity, and the stiffness of springs is assumed to be μ.

Let u_n be the displacement of the n-th node within the chain, with the unit interatomic spacing ($b = 1$). Then the equations of motion take the form

$$M\ddot{u}_n = \mu(u_{n+1} + u_{n-1} - 2u_n) \quad \text{with } n \text{ being integer.} \tag{17}$$

If the motion is time harmonic then $u_n = U_n \exp(-i\omega t)$, and therefore

$$-M\omega^2 U_n = \mu(U_{n+1} + U_{n-1} - 2U_n). \tag{18}$$

In the case of travelling waves, we have

$$U_n = U e^{inK}, \quad \text{with } U = \text{const}, \tag{19}$$

and the equation of motion becomes

$$-\omega^2 M U_n = 2\mu U_n(\cos(K) - 1).$$

The quantity K is said to be the Bloch parameter, and a solution u_n of (17), which satisfies the condition

$$u_{s+n} = u_s e^{inK},$$

is referred to as the *Bloch-Floquet wave*. A non-trivial solution U_n of (18), (19) exists, provided ω and K satisfy the following dispersion equation

$$\omega^2 - \frac{2\mu}{M}(1 - \cos(K)) = 0,$$

whose non-negative roots are

$$\omega = 2\sqrt{\frac{\mu}{M}}|\sin(K/2)|. \tag{20}$$

The corresponding dispersion curve, representing a periodic function of period 2π, is shown in Fig. 3. When the separation between the neighbouring particles equals b, the period for the dispersion curve becomes $2\pi/b$. The interval $(-\pi/b, \pi/b)$ is known as the *irreducible Brillouin zone*. Conventionally the dispersion diagrams are displayed for the values of K from the irreducible Brillouin zone. In the case when the "interatomic spacing" in the lattice equals b, the dispersion equation (20) is modified as follows:

$$\omega = 2\sqrt{\frac{\mu}{M}}|\sin\left(\frac{Kb}{2}\right)|. \tag{21}$$
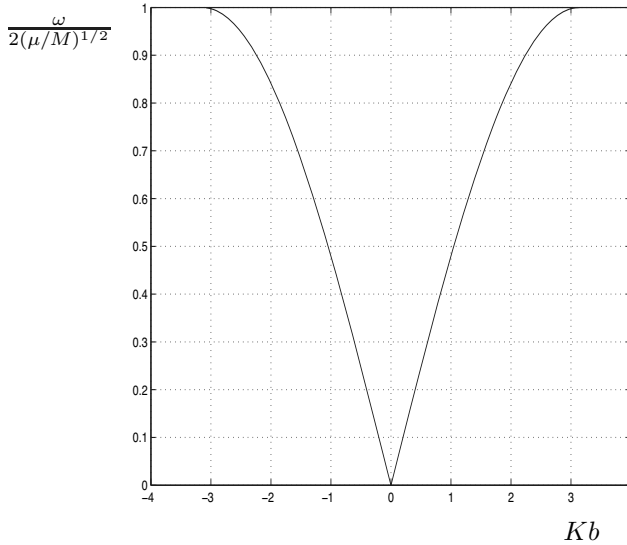
Figure 3. Dispersion diagram for a uniform spring-mass structure

Standing waves and "long-wave" asymptotic estimates

It is convenient to refer to the general case of an arbitrary interatomic separation b within the lattice. In particular, taking $b \to 0$ one obtains the continuum limit. We note that

$$U_{n+1}/U_n = e^{iKb},$$

and within the irreducible Brillouin zone we have $K_{max} = \pi/b$. In the continuum limit, as $b \to 0$, we deduce $K_{max} \to \infty$.

The transmission velocity of a wave packet is called the *group velocity*, and it is given as

$$v_g = \frac{d\omega}{dK} = \sqrt{\frac{\mu}{M}}\, b \cos(Kb/2).$$

On the boundaries $K = \pm\pi/b$ of the Brillouin zone, we have $v_g = 0$; the solution U_n represents a *standing wave* with zero net transmission velocity, and $U_n = (-1)^n U$.

In many physical applications, it is useful to have asymptotic approximations corresponding to the *long wave limit*. In particular, this will

give the slope of the curve $\omega = \omega(K)$ as $K \to 0+$, which is also referred to as the effective group velocity v_{eff} often used in *homogenization* approximations of wave phenomena in structured media. When $Kb \ll 1$, we have $\cos(Kb) \simeq 1 - \frac{1}{2}(Kb)^2$, and hence $\omega^2 \simeq \frac{\mu}{M}(Kb)^2$. Hence, $v_{\text{eff}} = (\mu/M)^{1/2}b$, and thus v_{eff} is frequency-independent in this limit.

A bi-atomic chain and stop bands

As a classical example (see, for example, Kittel (1996) and Brillouin (1953)), the one-dimensional periodic lattice consisting of two types of particles, of different masses, gives a very good illustration of filtering properties of structured media.

      Compared to the previous section, the new periodic system has two types of masses, M_1 and M_2, and springs of the normalized stiffness μ (see Fig. 4).
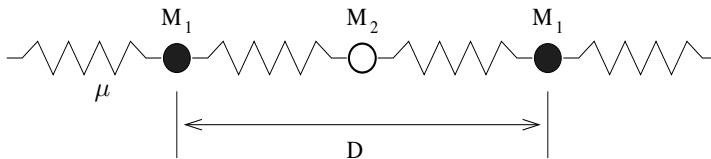
Figure 4. The one-dimensional "bi-atomic" periodic structure.

      In this case the elementary cell of the periodic lattice includes two different particles, with displacements u_n and v_n, and one needs two equations of motion as follows

$$M_1 \frac{d^2 u_n}{dt^2} = \mu(v_n + v_{n-1} - 2u_n), \ M_2 \frac{d^2 v_n}{dt^2} = \mu(u_{n+1} + u_n - 2v_n), \quad (22)$$

Let D be the size of the elementary cell, which is equal to the distance between the nearest particles of the same mass. Travelling waves are defined by

$$u_n = Ue^{i(nKD-\omega t)}, \ \ v_s = Ve^{i(nKD-i\omega t)},$$

where K is the wave number. On substitution into the equations of motion, we have

$$\omega^2\mu^{-1}M_1 U + V(1+e^{-iKD}) - 2U = 0, \ \omega^2\mu^{-1}M_2 V + U(1+e^{iKD}) - 2V = 0.$$

This is a homogeneous system of linear algebraic equations with respect to U and V, and it has a non-trivial solution if and only if

$$\frac{M_1 M_2}{\mu^2}\omega^4 - \frac{2(M_1 + M_2)}{\mu}\omega^2 + 2(1 - \cos(KD)) = 0. \tag{23}$$

This is the *dispersion equation* providing the relation between ω and K. For the present simple system, this equation has the explicit solution

$$\omega^2 = \mu\frac{M_1 + M_2 \pm \sqrt{(M_1 + M_2)^2 - 2M_1 M_2(1 - \cos(KD))}}{M_1 M_2}. \tag{24}$$

This formula suggests that the corresponding dispersion diagram, constructed for equation (23) has two branches. They are referred to as the "acoustic branch" (for the sign "-" in (24)) and the "optical branch" (for the sign "+" in (24)), as shown in Fig. 5.

We note that for the non-homogeneous system, when $M_1 \neq M_2$, there is a non-zero separation between the dispersion curves, a *stop band*. The width of the stop band can be computed by evaluating the frequencies at the end points of the Brillouin zone. At the boundary of the Brillouin zone, when $K = \pm\pi/a$, the roots of the dispersion equation are defined by

$$\omega^2 = \frac{\mu}{M_1 M_2}\{M_1 + M_2 \pm |M_1 - M_2|\}.$$

Assuming that $M_1 < M_2$, one can deduce that the width of the band gap is equal to $\sqrt{2\mu/M_1} - \sqrt{2\mu/M_2}$. If we fix M_2 and let the contrast parameter $r = M_2/M_1$ increase, then the width of the stop band will increase. No propagating wave exists within the interval of frequencies $(\sqrt{2\mu/M_2}, \sqrt{2\mu/M_1})$.

By looking at the dispersion diagram in Fig. 5, we can also identify the *high frequency stop band* defined as the interval $(\omega_*, +\infty)$, where $\omega_* = 2\mu(\frac{1}{M_1} + \frac{1}{M_2})$ is the upper limit for frequencies corresponding the optical branch of the dispersion diagram, obtained as $K \to 0$.

For the bi-atomic lattice system, the Bloch-Floquet waves exist only within the frequency intervals $[0, \sqrt{2\mu/M_2}]$ and $\left[\sqrt{2\mu/M_1}, \sqrt{2\mu(\frac{1}{M_1} + \frac{1}{M_2})}\right]$, which are also called the *pass-band* intervals; one can control the size of the pass-band intervals by changing the stiffness of springs and the masses of particles.
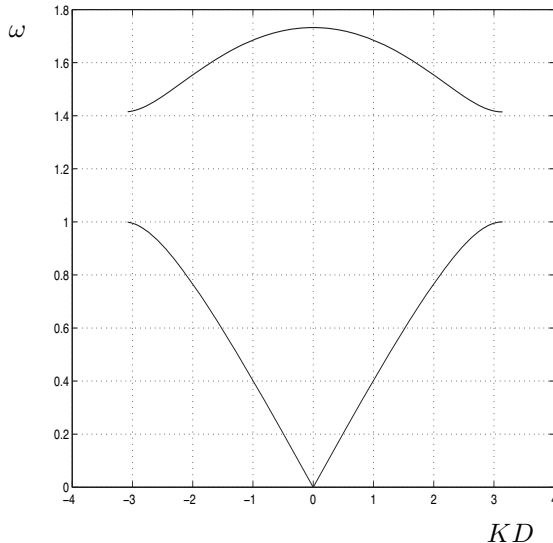
Figure 5. Dispersion curves for the "bi-atomic" spring-mass structure; in this computation $M_1 = 1, M_2 = 2, \mu = 1$.

0.4 Lattice approximation for continuous structured media

As we have demonstrated in the above section, the whole pass-band set, incorporating all pass-band intervals for a discrete periodic lattice, is bounded. In contrast, a continuum system would support propagation of high-frequency waves. For high-contrast periodic structures it is sometimes possible to construct a "lattice approximation", which would describe adequately the dispersion properties of Bloch-Floquet waves in the low frequency range. An example of such a structure is discussed in this section, which is based on the paper by Movchan *et al.* (2002b).

Instead of a discrete system of masses connected by weightless springs, we consider here a one-dimensional periodic array of elastic rods of different stiffness μ_j, $j = 1, 2$, and non-zero mass density, as shown in Fig. 6. For convenience, it is assumed that the linear mass density ρ is the same for all elements of this structure. Thus, the elementary cell contains two types of elastic rods. We use the notations $S_1^{(n)} = (-b + nD, nD)$, $S_2^{(n)} = (nD, a + nD)$, where n is integer, and $D = a + b$ is the total size of the

elementary cell.

Assuming that the waves are time-harmonic, of the radian frequency ω, we deduce that the amplitudes of the longitudinal displacements $U_j(x)$, $j = 1, 2$, satisfy the equations

$$\mu_j U_j'' + \omega^2 \rho U_j = 0, \quad x \in S_j^{(n)}, \ j = 1, 2. \tag{25}$$

The ideal contact conditions at the interface between two neighbouring rods imply

$$U_1 = U_2, \quad \mu_1 U_1' = \mu_2 U_2'. \tag{26}$$

The solution is sought in the class of Bloch-Floquet waves, for which we can write

$$U_j(x + D) = e^{iKD} U_j(x), \ j = 1, 2, \ |K| < \pi/D, \tag{27}$$

where K is the Bloch parameter.

The general solution of (25) is $U_j = A_j e^{ik_j x} + B_j e^{-ik_j x}$, $x \in S_j^{(n)}$, $j = 1, 2$, where A_j, B_j, $j = 1, 2$, are constant coefficients, and $k_j(\omega) = \omega\sqrt{\rho/\mu_j}$, $j = 1, 2$, are linear functions of ω. The interface conditions (26) and the Bloch-Floquet's condition (27), written for displacements within the elementary cell, lead to a homogeneous system of linear algebraic equations with respect to A_j, B_j, $j = 1, 2$:

$$\mathbf{Q}(K, \omega) \begin{pmatrix} A_1 \\ B_1 \\ A_2 \\ B_2 \end{pmatrix} = 0, \tag{28}$$

where

$$\mathbf{Q}(K, \omega)$$

$$= \begin{pmatrix} 1 & 1 & -1 & -1 \\ \mu_1 k_1 & -\mu_1 k_1 & -\mu_2 k_2 & \mu_2 k_2 \\ -e^{i(KD - k_1 b)} & -e^{i(KD + k_1 b)} & e^{ik_2 a} & e^{-ik_2 a} \\ k_1 e^{i(KD - k_1 b)} & -k_1 e^{i(KD + k_1 b)} & -\frac{\mu_2}{\mu_1} k_2 e^{ik_2 a} & \frac{\mu_2}{\mu_1} k_2 e^{-ik_2 a} \end{pmatrix}. \tag{29}$$

This system has a non-trivial solution, provided

$$\det \mathbf{Q}(K, \omega) = 0, \tag{30}$$

which relates the radian frequency ω to the Bloch parameter K and hence gives the dispersion equation for Bloch-Floquet waves propagating along the

periodic structure. It is convenient to introduce the notation $\varepsilon = \mu_1/\mu_2$, and in this case $k_2 = k_1\sqrt{\epsilon}$. Then (30) leads to

$$(\epsilon+1)\sin(k_1 b)\sin(k_1 a\sqrt{\epsilon}) - 2\sqrt{\epsilon}(\cos(k_1 b)\cos(k_1 a\sqrt{\epsilon}) - \cos(KD)) = 0. \quad (31)$$

The dispersion diagram, which shows ω versus K, is given in Fig. 7.

Let $\epsilon \ll 1$ and $k_1 b \ll 1$, i.e. the structure has the high-contrast in stiffness for different components, and the elastic rods of length b are relatively "short". Then the corresponding trigonometric parts in the left-hand side of (31) can be expanded into power series, and after truncation we obtain a polynomial expression in powers of ω.

Retaining the terms up to ω^4, we obtain the *approximate dispersion equation*

$$\omega^4 \mathcal{P} - \omega^2 \mathcal{Q} + 2(1 - \cos(KD)) = 0, \quad (32)$$

where the quantities $\mathcal{P}$ and $\mathcal{Q}$ are positive and have the form

$$\mathcal{P} = \frac{\rho^2}{12/\mu_1^2}(\epsilon a^2 + 2\epsilon ba + b^2)(\epsilon a^2 + b^2 + 2ba), \quad \mathcal{Q} = \frac{\rho}{\mu_1}(a+b)(\epsilon a + b).$$

Remarkably, equation (32) has the same structure as (23) derived for a discrete system incorporating a one-dimensional array of masses M_1, M_2 connected by elastic springs of stiffness μ. This observation suggests that a discrete lattice system can be used to approximate a high-contrast periodic continuous systems to obtain its dynamic response within the low frequency range.

This discrete model can be characterised by the two parameters M_1/μ and M_2/μ, and the equations (32) and (23) become the same when

$$\mathcal{P} = M_1 M_2/\mu^2, \quad \mathcal{Q} = 2(M_1 + M_2)/\mu.$$

Of course, in this case the dispersion diagrams, within the range of frequencies covering the acoustic and optical branches, also agree. In the dispersion diagram of Fig. 7 we show the dependance of k_1 versus K and note the presence of stop bands, which occur for Bloch waves in the high-contrast bi-material periodic system. For this computational example we used the following numerical values of the geometrical and materials parameters: $D = 1, b = 0.5, \epsilon = 0.1$.

It is noted that an infinite number of dispersion curves corresponds to the bi-material continuum system, whereas the lattice approximation covers only first two dispersion curves adjacent to the origin.
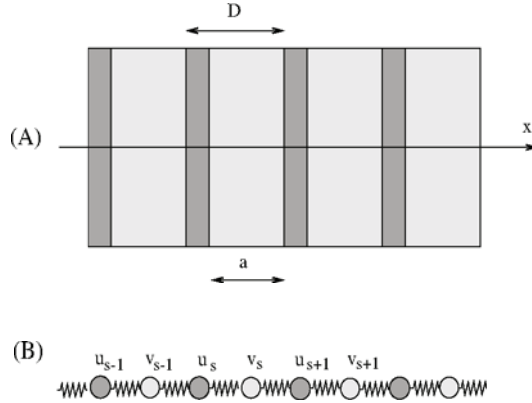
Figure 6. One-dimensional arrays of two layers (A) and the approximating periodic lattice system of two types of particles connected by springs (B).

0.5 Transmission through a finite thickness interface

We can consider a one-dimensional "structured interface", which incorporates a finite number of elastic rods aligned with the x−axis and joined together sequentially. The rods themselves may have different lengths, densities and elastic stiffness. A wave propagating in the positive direction of the x−axis interacts with the interface, and some of the energy gets reflected whereas the remaining energy is transmitted through the interface. The percentage of the reflected energy is frequency dependent. For the case when there is a repeating pattern, and the size of such an interface increases to infinity to form a periodic structure, it is appropriate to make a connection with analysis of Bloch-Floquet waves and their dispersion properties in the periodic system, as explained in Lekner (1994) and Brun *et al.* (2010a). However, when the thickness of the interface structure is not large, the analysis follows a different pattern. The emphasis is on trapped modes, which may exist within the structured interface and which may enhance its transmittance properties. The transmission matrix technique, as in Lekner (1994), is an efficient tool outlined below.

The displacement amplitude u for the time-harmonic motion of ra-
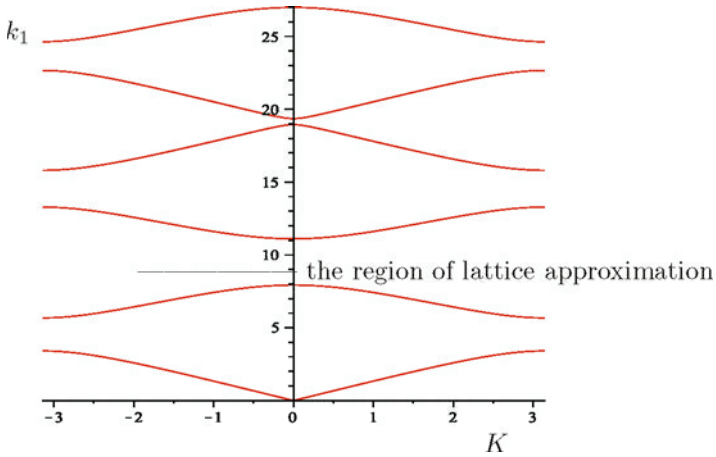
Figure 7. Dispersion diagram for Bloch waves in the high-contrast bi-material periodic system.

dian frequency ω satisfies the equation

$$\frac{\partial^2 u(x)}{\partial x^2} + \frac{\rho}{\mu}\omega^2 u(x) = 0, \tag{33}$$

where ρ and μ are the mass density and the stiffness constants, respectively. The wave form can be expressed in terms of complex amplitudes A and B

$$u(x) = A\exp(ikx) + B\exp(-ikx), \tag{34}$$

with

$$k = \omega c, \quad c = \sqrt{\frac{\rho}{\mu}}.$$

Consider a one-phase interface located at $x = x_0$ and $x = x_1 = x_0 + d$. Then displacements and tractions are related by

$$\begin{bmatrix} u(x_1) \\[2mm] \mu\dfrac{\partial u}{\partial x}(x_1) \end{bmatrix} = \begin{bmatrix} m_{11} & m_{12} \\[2mm] m_{21} & m_{22} \end{bmatrix} \begin{bmatrix} u(x_0) \\[2mm] \mu\dfrac{\partial u}{\partial x}(x_0) \end{bmatrix}, \tag{35}$$

where, according to (34), we have

$$\mathbf{M} = \begin{bmatrix} \cos\delta & \dfrac{\sin\delta}{Q} \\ -Q\sin\delta & \cos\delta \end{bmatrix}, \tag{36}$$

with $Q = \mu\,k$ and $\delta = k\,d$ being the *phase increment*. The matrix $\mathbf{M}$ in (36) is said to be the *transfer matrix* and its eigenvalues are

$$\cos\delta \pm \sqrt{\cos^2\delta - 1} = \exp(\pm i\delta). \tag{37}$$

Along the same lines, we now analyse a *discrete interface* consisting of two springs of stiffness γ and and a mass m. The transfer matrix $\mathbf{M}^{(d)}$ of the discrete interface is defined in the form

$$\mathbf{M}^{(d)} = \begin{bmatrix} \dfrac{\gamma - m\omega^2}{\gamma} & \dfrac{2\gamma - m\omega^2}{\gamma^2} \\ -m\omega^2 & \dfrac{\gamma - m\omega^2}{\gamma} \end{bmatrix}. \tag{38}$$

The eigenvalues of the transfer matrix (38) are

$$1 - \frac{m}{\gamma}\omega^2 \pm \sqrt{\frac{m}{\gamma}\omega^2\left(\frac{m}{\gamma}\omega^2 - 2\right)}, \tag{39}$$

so that the dependence on ω is algebraic for the structured discrete interface, in contrast with the continuum one-phase interface (see (37)). It is also noted that the eigenvalues (39) are complex for sufficiently small ω and real when ω is sufficiently large.

If several interface regions, continuous or discrete, are placed together to form an interface stack then the transfer matrix is obtained by the appropriate multiplication of the transfer matrices of individual layers within the stack, as discussed in Brun *et al.* (2010a).

Reflected and transmitted energy

We consider an interface stack with the overall 2×2 transfer matrix $\mathbf{M} = (m_{ij})$ separating two elastic media (for the one dimensional case, we have two semi-infinite elastic rods located along the intervals $x < x_0$ and $x > x_1$), with the density ρ_- and stiffness μ_- on the left from the interface and the

density ρ_+ and stiffness μ_+ on the right from the interface. The *incident* and *reflected* waves on the left of the interface admit the representation

$$u(x) = A_I \exp(ik_- x) + A_R \exp(-ik_- x), \qquad (40)$$

where A_I and A_R are the *incident* and *reflection amplitudes*, while the transmitted wave on the right of the interface is given by

$$u(x) = \sqrt{\frac{\mu_-}{\mu_+}} A_T \exp(ik_+ x), \qquad (41)$$

with A_T denoting the *transmission amplitude*, and $k_\pm$ standing for the corresponding wave numbers in the regions outside the interface.

According the definition of the transfer matrix outlined in the text above, the coefficients A_R, A_T and A_I satisfy the equation

$$\sqrt{\frac{\mu_-}{\mu_+}} \left[\begin{array}{c} A_T e^{ik_+ x_1} \\ iQ_+ A_T e^{ik_+ x_1} \end{array} \right] = \mathbf{M} \left[\begin{array}{c} A_I e^{ik_- x_0} + A_R e^{-ik_- x_0} \\ iQ_-(A_I e^{ik_- x_0} - A_R e^{-ik_- x_0}) \end{array} \right], \qquad (42)$$

where $Q_\pm = \mu_\pm k_\pm$. In turn, the amplitudes A_R and A_T of the reflected and transmitted waves can be written (see Brun *et al.* (2010a)) in the form

$$\bar{A}_R = \frac{Q_- Q_+ m_{12} + m_{21} + i(Q_- m_{22} - Q_+ m_{11})}{Q_- Q_+ m_{12} - m_{21} + i(Q_- m_{22} + Q_+ m_{11})} e^{2ik_- x_0},$$

$$\bar{A}_T = \sqrt{\frac{\mu_+}{\mu_-}} \frac{2iQ_-}{Q_- Q_+ m_{12} - m_{21} + i(Q_- m_{22} + Q_+ m_{11})} e^{i(k_- x_0 - k_+ x_1)},$$

$$\qquad (43)$$

where we have used the normalised quantities $\bar{A}_R = A_R/A_I$, $\bar{A}_T = A_T/A_I$.

According to the standard procedure, as in Lekner (1994) and Brun *et al.* (2010a), the normalized *reflected* R and *transmitted* $T = 1 - R$ energies are given by

$$R = |\bar{A}_R|^2 = \frac{(Q_- Q_+ m_{12} + m_{21})^2 + (Q_- m_{22} - Q_+ m_{11})^2}{(Q_- Q_+ m_{12} - m_{21})^2 + (Q_- m_{22} + Q_+ m_{11})^2},$$

$$T = |\bar{A}_T|^2 \frac{Q_+}{Q_-} = \frac{4Q_- Q_+}{(Q_- Q_+ m_{12} - m_{21})^2 + (Q_- m_{22} + Q_+ m_{11})^2}, \qquad (44)$$

so that the total transmission corresponds to the case of $R = 0$, $T = 1$, and total reflection corresponds to $R = 1$, $T = 0$.

Defect modes and enhanced transmission

There is a connection between the transmission properties of a finite width stack and dispersion properties of Bloch waves in infinite doubly periodic

plane. In particular, if a full stop band is identified for Bloch waves, then the the finite width stack built of the same material is expected to reflect the bulk of the energy within the stop band frequency range. However, the presence of defects in the stack may alter its transmission properties. This is illustrated here for a simple one-dimensional example.

We consider the one-dimensional problem involving the spring-mass interface, as described above. In the computational example below, the discrete interface is composed of masses $m = 387.3kg$ and $M = 3m$ connected be identical springs of stiffness $\gamma = 3873N/m$. The dispersion diagram, which shows the wave number versus the radian frequency, for the two mass lattice system is given in Fig. 8. As expected, this diagram includes the band gap. If a finite sample $mM - mM - mM - mM$ of this periodic system is used as a structured interface, the bulk of the energy would be reflected within the stop band frequency range.
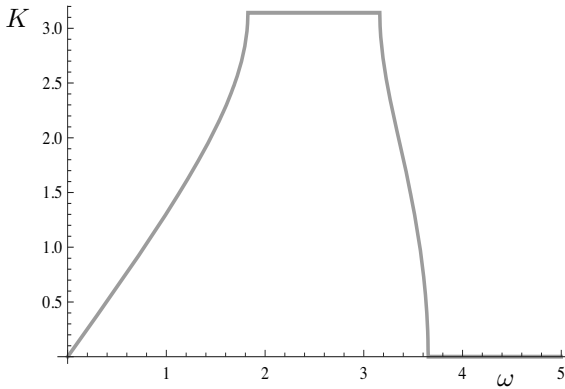
Figure 8. Dispersion diagram for discrete system of masses m and M connected by springs of stiffness γ.

The plot of the normalized reflected energy as a function of the frequency are shown (in gray colour) in Fig. 9 where the bi-atomic lattice interface $mM - mM - mM - mM$ is inserted between two different infinite continuous media. The continuous media on the left and on the right from the interface have the elastic impedance $\sqrt{\rho_-\mu_-} = 100Pa/m$ and $\sqrt{\rho_+\mu_+} = 1500Pa/m$, respectively.

On the same figure, we also show (black curve) the normalised reflected energy for the interface $mM - Mm - mM - mM$, where a defect has
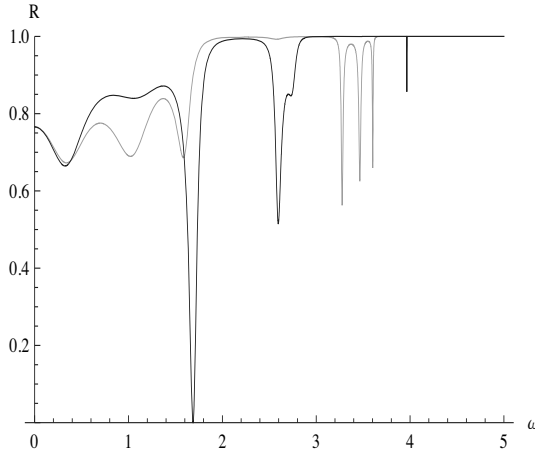
Figure 9. Normalised reflected energy for the stack consisting of 4 cells, mM-Mm-mM-mM (black curve), versus the normalised reflected energy for the stack mM-mM-mM-mM (gray curve).

been created by changing the order of masses M and m in the second cell of the stack. This change leads to an enhanced transmission (i.e. a sharp drop in the reflected energy), which is clearly visible on the diagram in Fig. 9. This effect is discussed in detail in the next section, where localisation, associated with "defect modes" within a structured interface, is shown to lead to an enhanced transmission.

## 0.6 Polarisation and enhanced transmission of elastic waves by a shear-type structured interface

This section reviews the results of the paper by Brun *et al.* (2010b) addressing a vector problem of two-dimensional elasticity incorporating plane pressure and shear waves interacting with a finite width structured interface of shear type. The emphasis is on the formation of the defect modes within the interface, which lead to an enhanced transmission. For this configuration, we also discuss the wave polarisation as a result of the interaction with the structured interface

Structured interface in an elastic medium

The structured interface is assumed to occupy a horizontal strip in the (x, z)-plane:

$$\Pi_D = \{(x, z) : x \in \mathbb{R}, -D \leq z \leq 0\}. \tag{45}$$

We consider an example where the structure within the interface includes three parallel elastic infinite bars connected by transverse elastic massless links. In other words, within the interface we have an elastic frame, so that the angle between the vertical links and the horizontal elastic bars is maintained at $\pi/2$. The notations $\Omega_\pm$ are used for the half-planes above and below the structured interface. The sketch of the elastic system and relevant notations are shown in Fig. 10.
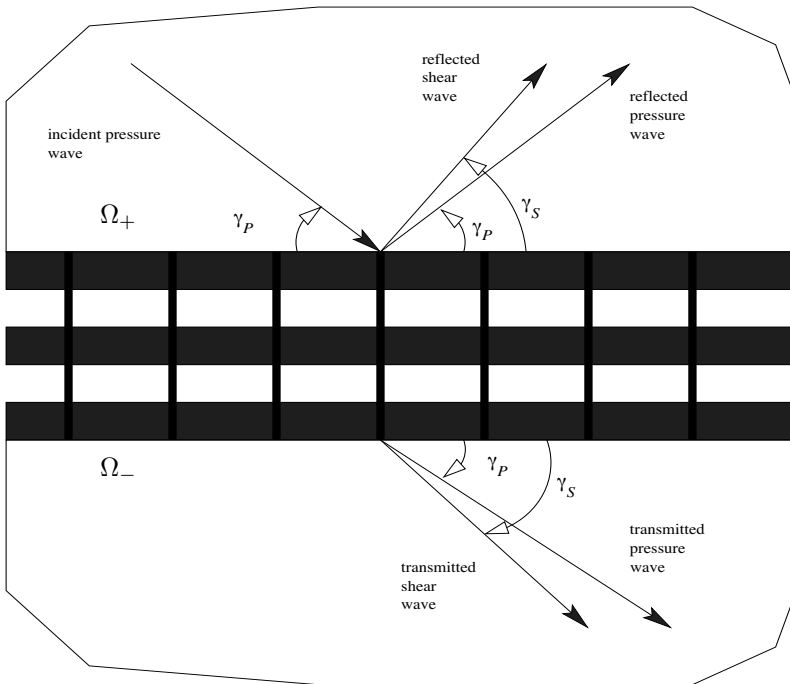
Figure 10. Structured shear-type interface, separating the elastic half-planes $\Omega_\pm$.

Each elastic bar $l_j, j = 1, 2, 3$, is assumed to be of high flexural stiffness and hence is approximated as as a one-dimensional elastic element, which moves only in the horizontal direction (along the Ox-axis), with the elastic displacement $\mathbf{u}^{(j)} \sim u_j(x, t)\mathbf{e}^{(1)}$. The equations of motion can be written separately for the elastic bar inside the interface $(j = 2)$, and for the bars adjacent to Ω_+ and Ω_- $(j = 1$ and $j = 3)$. The equation of motion for the interior bar is

$$E(u_2)_{xx} - \rho(u_2)_{tt} - 2\gamma u_2 + \gamma(u_3 - u_1) = 0, \tag{46}$$

where $(u_j)_{xx}$ and $(u_j)_{tt}$ stand for the second-order partial derivatives with respect to x and t, respectively.

For the bars forming the boundary of the structured interface, the equations of motion are

$$E(u_1)_{xx} - \rho(u_1)_{tt} + \gamma(u_2 - u_1) + \tau_+ = 0, \tag{47}$$

$$E(u_3)_{xx} - \rho(u_3)_{tt} + \gamma(u_2 - u_3) - \tau_- = 0. \tag{48}$$

Here τ_+ and τ_- are the shear stresses in the ambient elastic media above and below the interface.

Elastic waves in the ambient medium

The upper half-plane Ω_+ includes the incident plane pressure wave, together with reflected pressure and shear waves. The transmitted pressure and shear waves propagate in the lower half-palne Ω_-. Taking the $x-$axis along the interface, $z-$axis perpendicular to the interface and $y-$axis to be pointed out of the plane of Fig. 10, we use the standard representation of the displacement

$$u(x, z, t)\mathbf{e}^{(1)} + w(x, z, t)\mathbf{e}^{(3)}$$

in terms of the scalar and vector potentials $\varphi(x, z, t)$ and $\psi(x, z, t)\mathbf{e}^{(2)}$:

$$u = \frac{\partial \varphi}{\partial x} - \frac{\partial \psi}{\partial z}, \quad w = \frac{\partial \varphi}{\partial z} + \frac{\partial \psi}{\partial x}. \tag{49}$$

The notations $\{\varphi^{(I)}, \psi^{(I)}\}$, $\{\varphi^{(R)}, \psi^{(R)}\}$, $\{\varphi^{(T)}, \psi^{(T)}\}$ correspond to the incident, reflected and transmitted waves, respectively. Since the incident wave is assumed to be of pressure type, we have $\psi^{(I)} \equiv 0$.

Assume that the same elastic material occupies Ω_+ and Ω_-. If α, β are the wave speeds of the pressure and shear waves then the pressure and shear wave potentials ϕ and ψ in the elastic continuum satisfy the wave equations

$$\triangle\varphi - \frac{1}{\alpha^2}\frac{\partial^2}{\partial t^2}\varphi = 0, \qquad \triangle\psi - \frac{1}{\beta^2}\frac{\partial^2}{\partial t^2}\psi = 0, \tag{50}$$

where

$$\alpha = \sqrt{\frac{\lambda + 2\mu}{\rho}}, \qquad \beta = \sqrt{\frac{\mu}{\rho}}. \qquad (51)$$

Let c be an apparent velocity of the incident pressure wave along the horizontal interface, and let $\chi_P \in [0, \pi/2]$ and $\chi_S \in [0, \pi/2]$ denote the angle between the direction of the incident or transmitted pressure wave and the horizontal interface and the angle between the direction of propagation of the reflected or transmitted shear wave and the horizontal interface. Then

$$a := \tan \chi_P = \sqrt{\frac{c^2}{\alpha^2} - 1} \ \ \text{and} \ \ b := \tan \chi_S = \sqrt{\frac{c^2}{\beta^2} - 1}. \qquad (52)$$

For the pressure wave, the angle of reflection is equal to the angle of incidence, and $\chi_S > \chi_P$ (see Fig. 10).

Accordingly, the pressure and shear wave potentials are

$$\begin{aligned} \varphi_+ = \ \ \varphi^{(I)} + \varphi^{(R)} = \ \ & A_I \exp[ik(ct - x + az)] + A_R \exp[ik(ct - x - az)], \\ \psi_+ = \ \ \psi^{(R)} = \ \ & B_R \exp[ik(ct - x - bz)], \end{aligned} \qquad (53)$$

in Ω_+, and

$$\begin{aligned} \varphi_- = \ \ \varphi^{(T)} = \ \ & A_T \exp[ik(ct - x + az)], \\ \psi_- = \ \ \psi^{(T)} = \ \ & B_T \exp[ik(ct - x + bz)], \end{aligned} \qquad (54)$$

in Ω_-. Here

$$k = \frac{2\pi}{\Lambda_P} \cos \chi_P = \frac{2\pi}{\Lambda_S} \cos \chi_S, \qquad (55)$$

where Λ_P and Λ_S are the wave lengths of the pressure and shear waves in the ambient elastic medium $\Omega_+ \cup \Omega_-$, and $\omega = kc$ is the radian frequency.

It is assumed that the amplitude A_I of the incident pressure wave is given, whereas A_R, B_R, A_T, B_T are evaluated with the account of the structured interface. In the text below, special attention is given to an enhanced transmission corresponding to a class of trapped modes which may occur within the interface structure.

The energy balance

Assuming that the motion is time-harmonic with the radian frequency ω, we use the notations U_j and $T_\pm$ for the amplitudes of the displacements of the bars $l_j, j = 1, 2, 3$ and for the shear stresses above and below the interface.

Then the equations of motion of elastic bars within the shear-type interface lead to the algebraic system

$$\mathcal{R}\mathbf{U} = \mathbf{T}, \tag{56}$$

where

$$\mathbf{U} = (U_1, U_2, U_3)^T, \ \mathbf{T} = (-T_+, 0, T_-)^T, \tag{57}$$

and

$$\mathcal{R} = \begin{pmatrix} -\Gamma & \gamma & 0 \\ \gamma & -\Gamma - \gamma & \gamma \\ 0 & \gamma & -\Gamma \end{pmatrix}, \tag{58}$$

with $\Gamma = k^2 E + \gamma - \rho\omega^2$.

As described in Brun *et al.* (2010b), the standard procedure involves the Betti formula applied to the displacement and its complex conjugate above and below the interface. Furthermore, using the plane wave representations (53) and (54) that include the pressure and shear wave potentials we deduce the following energy balance relation

$$E_I = E_R + E_T, \tag{59}$$

where

$$E_I = a|A_I|^2, E_R = a|A_R|^2 + b|B_R|^2, E_T = a|A_T|^2 + b|B_T|^2, \tag{60}$$

E_I, E_R and E_T represent the vertical energy fluxes of the incident, reflected and transmitted fields, respectively.

The effect of the interface on the distribution of energy can be seen by the evaluation of the coefficients A_R, B_R and A_T, B_T characterising the reflected and transmitted fields.

Trapped modes within the structured interface

Trapped vibrations within the structured interface can significantly alter its transmission properties. In the particular case involving the three-bar interface we discuss several examples in this section.

For a non-resonant regime, when $\det \mathcal{R} \neq 0$, the system (56) has a solution

$$\begin{pmatrix} U_1 \\ U_2 \\ U_3 \end{pmatrix} = \mathcal{R}^{-1} \begin{pmatrix} -T_+ \\ 0 \\ T_- \end{pmatrix}, \tag{61}$$

where

$$\mathcal{R}^{-1} = \frac{1}{(\gamma - \Gamma)(2\gamma + \Gamma)} \begin{pmatrix} \gamma - \frac{\gamma^2}{\Gamma} + \Gamma & \gamma & \frac{\gamma^2}{\Gamma} \\ \gamma & \Gamma & \gamma \\ \frac{\gamma^2}{\Gamma} & \gamma & \gamma - \frac{\gamma^2}{\Gamma} + \Gamma \end{pmatrix}. \qquad (62)$$

In particular, the effective transmission relations for the shear displacements and shear stresses across the structured interface have the form:

$$U_1 = \frac{\frac{\gamma^2}{\Gamma}(T_+ + T_-) - T_+(\gamma + \Gamma)}{(\gamma - \Gamma)(2\gamma + \Gamma)},$$

$$U_3 = \frac{T_-(\gamma + \Gamma) - \frac{\gamma^2}{\Gamma}(T_+ + T_-)}{(\gamma - \Gamma)(2\gamma + \Gamma)}. \qquad (63)$$

Solving the above system of algebraic equations with respect to B_R, B_T we deduce that

$$B_R = -\frac{2a}{\Psi} \left[\Phi(\Gamma^2 + \gamma\Gamma - \gamma^2) - \gamma^2\Gamma(1 + ab) \right] A_I,$$

$$B_T = \frac{2ia^2(1 + b^2)}{\Psi} k\gamma^2\mu e^{ibDk} A_I, \qquad (64)$$

where $\Psi = \Gamma(1 + ab) + ik\mu a(1 + b^2)$ and $\Phi = \Psi\left[(\gamma + \Gamma)\Phi - 2\gamma^2(1 + ab)\right]$. The conditions of zero transverse displacements at the interface lead to the expressions for the coefficients A_R, A_T as follows

$$A_R = A_I - a^{-1}B_R, \qquad A_T = a^{-1}B_T e^{-ik(b-a)D}, \qquad (65)$$

The full set $\{A_R, B_R, A_T, B_T\}$ determines the reflected and transmitted waves at the shear-type interface.

Furthermore, the system (56) can be written as follows

$$\mathbf{B} \begin{pmatrix} [[U]] \\ [[V]] \\ \langle U \rangle \end{pmatrix} = \begin{pmatrix} T_+ + T_- \\ \frac{1}{2}(T_- - T_+) \\ \frac{1}{3}(T_- - T_+) \end{pmatrix}, \qquad (66)$$

where $[[U]] = U_3 - U_1$ represents the tangential displacement jump across the interface, $[[V]] = \frac{1}{2}(U_3 + U_1) - U_2$ is the average jump representing the difference between the average tangential displacement on the boundary and the tangential displacement of the interior bar, $\langle U \rangle = \frac{1}{3}(U_1 + U_2 + U_3)$ is the average tangential displacement over the whole structured interface, and

$$\mathbf{B} = \mathrm{diag}\left\{-Ek^2 + \rho\omega^2 - \gamma, -Ek^2 + \rho\omega^2 - 3\gamma, -Ek^2 + \rho\omega^2\right\}. \qquad (67)$$

The relation between $([[U]], [[V]]), \langle U \rangle)^T$ and $(U_1, U_2, U_3)^T$ has the form

$$
\begin{pmatrix} [[U]] \\ [[V]] \\ \langle U \rangle \end{pmatrix} = \mathcal{Q} \begin{pmatrix} U_1 \\ U_2 \\ U_3 \end{pmatrix},
\tag{68}
$$

where

$$
\mathcal{Q} = \begin{pmatrix} -1 & 0 & 1 \\ \frac{1}{2} & -1 & \frac{1}{2} \\ \frac{1}{3} & \frac{1}{3} & \frac{1}{3} \end{pmatrix},
\tag{69}
$$

and hence

$$
\mathbf{B} = \mathcal{Q}\mathcal{R}\mathcal{Q}^{-1}.
\tag{70}
$$

The rows of the matrix $\mathcal{Q}$ are the eigenvectors of $\mathcal{R}$ corresponding to the eigenvalues, which coincide with the diagonal entries of the matrix $\mathbf{B}$, and

$$
\det \mathbf{B} = \det \mathcal{R}.
\tag{71}
$$

The relation

$$
\det \mathcal{R}(\omega, k) = 0
\tag{72}
$$

is the dispersion equation for the elastic waves propagating horizontally along the structured interface, which is equivalent to

$$
(-Ek^2 + \rho\omega^2 - \gamma)(-Ek^2 + \rho\omega^2 - 3\gamma)(-Ek^2 + \rho\omega^2) = 0.
\tag{73}
$$

The corresponding dispersion diagram has three branches shown in Fig. 11:

$$
\begin{aligned}
(1) & \qquad Ek^2 + 3\gamma - \rho\omega^2 = 0, \\
(2) & \qquad Ek^2 + \gamma - \rho\omega^2 = 0, \\
(3) & \qquad Ek^2 - \rho\omega^2 = 0.
\end{aligned}
\tag{74}
$$

The lowest branch (3) gives a linear relation between k and ω, which corresponds to a non-dispersive wave propagating along an elastic bar. For the dispersive waves (branches (1) and (2)), there is a cut-off frequency

$$
\omega^* = \sqrt{\frac{\gamma}{\rho}},
\tag{75}
$$

and for $\omega < \omega^*$ no dispersive wave can propagate along the interface.

The resonance states correspond to the cases where the frequency ω of the incident wave coincides with one of the solutions of the dispersion equation (73). For the three-bar interface, such states can be classified as follows: